Original Article

Long non-coding RNA MIR4435-2HG promotes pancreatic cancer progression by regulating ABHD17C through sponging miR-128-3p

Zhou Chen[1,2], Yan Du[3], Huaqing Shi[3], Shi Dong[3], Ru He[3], Wence Zhou[1,4]

[1]Department of General Surgery, The First School of Clinical Medicine, Lanzhou University, Lanzhou, China; [2]Department of General Surgery, The First Hospital of Lanzhou University, Lanzhou, China; [3]Department of General Surgery, The Second Clinical Medical School, Lanzhou University, Lanzhou, China; [4]Department of General Surgery, The Second Hospital & Clinical Medical School, Lanzhou University, Lanzhou, China

Contributions: (I) Conception and design: Z Chen, W Zhou; (II) Administrative support: Z Chen, W Zhou; (III) Provision of study materials or patients: Z Chen, Y Du, H Shi; (IV) Collection and assembly of data: Z Chen, Y Du, H Shi, S Dong, R He; (V) Data analysis and interpretation: Z Chen, Y Du, H Shi, S Dong, R He; (VI) Manuscript writing: All authors; (VII) Final approval of manuscript: All authors.

Correspondence to: Wence Zhou, MD, PhD. Department of General Surgery, The First School of Clinical Medicine, Lanzhou University, Lanzhou 730000, China; Department of General Surgery, The Second Hospital & Clinical Medical School, Lanzhou University, No. 80, Cuiyingmen, Chengguan District, Lanzhou 73000, China. Email: zhouwc129@163.com.

Background: The recently identified carcinogenic long non-coding RNA (lncRNA) MIR4435-2HG has been validated to contribute to the initiation and progression of several malignancies. Nonetheless, its specific mechanistic function in pancreatic cancer (PC) is yet to be determined. This study aims to investigate the expression and functional role of MIR4435-2HG in PC and to elucidate its potential mechanism.

Methods: This study employed The Cancer Genome Atlas (TCGA) and Genotype-Tissue Expression (GTEx)-Pancreas datasets for the analysis of MIR4435-2HG expression in PC and normal pancreatic tissues and its relations with prognosis in PC. Moreover, quantitative real-time polymerase chain reaction (qRT-PCR) was employed for analyzing MIR4435-2HG, miR-128-3p, and ABHD17C expressions within cells and tissues. Cell proliferation and apoptosis were detected *in vitro* through Cell Counting Kit 8 (CCK-8) assay and flow cytometry while utilizing transwell and wound healing assays to assess cell migration and invasion. Predicting miR-128-3p binding sites with MIR4435-2HG or ABHD17C was conducted via the online tool starBase and validated through a dual-luciferase reporter (DLR), RNA pull-down and RNA binding protein immunoprecipitation (RIP) assays. Herein, we deployed Western blot to assess protein expression levels. The *in vivo* role of MIR4435-2HG was studied using tumor xenografts.

Results: MIR4435-2HG overexpression exhibited a correlation with poor prognosis in PC. Knocking down MIR4435-2HG significantly hindered the proliferative, invading, and migrating PC cell abilities, accompanied by apoptosis induction, counteracted via a miR-128-3p inhibitor. Moreover, MIR4435-2HG could directly bind to miR-128-3p. Additionally, miR-128-3p directly targeted ABHD17C. Furthermore, *in vitro* as well as *in vivo* experiment results elucidated that knocking down MIR4435-2HG hindered PC progression by suppressing ABHD17C expression via miR-128-3p upregulation.

Conclusions: MIR4435-2HG can serve as a dependable target for PC diagnosis and treatment by modulating the miR-128-3p/ABHD17C axis to promote its progression.

Keywords: MIR4435-2HG; pancreatic cancer (PC); miR-128-3p; ABHD17C

Submitted Jan 09, 2024. Accepted for publication Jul 07, 2024. Published online Aug 23, 2024.
doi: 10.21037/tcr-24-51
View this article at: https://dx.doi.org/10.21037/tcr-24-51

Introduction

Pancreatic cancer (PC) represents a highly prevalent and fatal neoplasm affecting the digestive tract worldwide (1). PC onset is insidious, diagnosed at an advanced stage, and frequently accompanied by the presence of metastases to distant sites. PC survival time has improved to some extent recently, but the results remain unsatisfactory, with less than a 10% 5-year survival rate (2). The prevailing primary therapeutic approach for PC involves radical surgery. Nevertheless, it is worth noting that less than 20% of PCs meet the criteria for resection (3). Furthermore, patients with PC have a higher recurrence rate after surgery, and most die from metastasis (4). Patients with advanced PC have limited treatment options; therefore, new targets are required to effectively diagnose and manage PC.

Long non-coding RNAs (lncRNAs) are a non-protein-coding transcript class having a length exceeding 200 nucleotides (5,6). Dysregulated lncRNAs can result in abnormal gene expression, chemotherapy resistance and progression in various tumors (7,8). MIR4435-2HG, termed LINC00978, MORRBID, is a lncRNA located on chromosome region 2q13, comprising 10 exons (9,10). This lncRNA is crucial in driving tumor cell malignant behavior that includes proliferation, invasion, migration, and metastasis, besides being a prognostic biomarker for patients (11,12). Mechanistically, MIR4435-2HG can function as a microRNA (miRNA) sponge, thereby releasing its inhibitory effect on downstream target gene expression (13). MIR4435-2HG is overexpressed and enhances hepatocellular carcinoma (HCC) cell line proliferation by activating miR-487a (14). Furthermore, MIR4435-2HG exhibits overexpression in HCC and enhances SRY-box transcription factor 12 (SOX12) expression through sponge adsorption of miR-125-5p, thereby promoting HCC progression (15). MIR4435-2HG affects the ability of head and neck squamous cell carcinoma (HNSCC) to proliferate and migrate, besides affecting epithelial-mesenchymal transition (EMT) via miR-383-5p regulation (16). The probable miR-128-3p implication in tumor progression has been suggested through its ability to target various genes (17,18). However, the molecular mechanism behind MIR4435-2HG regulation in PC is yet to be clarified. The primary objective of this study is to elucidate the expression pattern and biological functions of MIR4435-2HG in PC. Additionally, we aim to investigate its role as a sponge, adsorbing miR-128-3p and consequently regulating the expression of the target gene ABHD17C. This, in turn, provides a novel therapeutic target for the treatment of PC. We present this article in accordance with the MDAR and the ARRIVE reporting checklists (available at https://tcr.amegroups.com/article/view/10.21037/tcr-24-51/rc).

Highlight box

Key findings

- MIR4435-2HG is significantly overexpressed in pancreatic cancer (PC) and correlates with poor prognosis. Knocking down MIR4435-2HG inhibits PC cell proliferation, invasion, and migration, and induces apoptosis. It directly binds to miR-128-3p, which targets ABHD17C, thereby regulating PC progression.

What is known and what is new?

- Long non-coding RNAs, including MIR4435-2HG, contribute to the development and progression of various cancers.
- This study elucidates the specific mechanism of MIR4435-2HG in PC, demonstrating its role in modulating the miR-128-3p/ABHD17C axis, thereby promoting PC progression.

What is the implication, and what should change now?

- MIR4435-2HG is a potential biomarker and therapeutic target for PC. Understanding its role in the miR-128-3p/ABHD17C axis provides new insights into PC treatment strategies.
- Clinical strategies should incorporate targeting MIR4435-2HG for PC diagnosis and therapy. Further research should focus on developing inhibitors for MIR4435-2HG and exploring its potential in PC.

Methods

RNA-seq and clinical downloaded data

This study was conducted in accordance with the Declaration of Helsinki (as revised in 2013). The Cancer Genome Atlas (TCGA)-pancreatic adenocarcinoma (PAAD) dataset included 178 PC and 4 normal pancreatic tissue samples, and the GTEx-Pancreas dataset included 167 normal pancreatic tissue samples. This study deployed the Wilcox test to evaluate MIR4435-2HG differential expression between tumor and normal tissues subsequent to integrating TCGA-PAAD and GTEx-Pancreas datasets. Clinical data that included overall survival (OS), disease-specific survival (DSS), progression-free interval (PFI), age, gender, histologic grade, and T/N/M stages were obtained from the TCGA database for 178 PC samples. Relying upon MIR4435-2HG median expression, we categorized the PC samples into high-expression and low-expression groups, followed by employing the Kaplan-Meier survival curve to compare the difference in survival time between

Table 1 MIR4435-2HG correlation to clinicopathological pancreatic cancer characteristics

Factor	No. patients	MIR4435-2HG expression		P value
		Low (n=26)	High (n=34)	
Gender				0.80
Female	22	10	12	
Male	38	16	22	
Age (years old)				0.40
≤60	24	12	12	
>60	36	14	22	
Tumor size (cm)				0.25
≤4	39	19	20	
>4	21	7	14	
Lymph node metastasis				0.04*
No	30	17	13	
Yes	30	9	21	
Vascular invasion				0.20
No	45	22	24	
Yes	15	4	10	
Nerve invasion				0.10
No	14	23	24	
Yes	46	3	10	
AJCC stage				0.04*
I–II	46	23	22	
III–IV	14	3	12	

*, P<0.05. AJCC, American Joint Committee on Cancer.

these two groups. Our study employed univariate and multivariate Cox analyses for assessing the risk factors for PC patient prognosis.

Clinical samples

Sixty pairs of PC and corresponding adjacent normal tissues were acquired from the First Hospital of Lanzhou University, and this study has been approved by its Institutional Review Board (IRB) (approval number: LDYYLL2022-505), the informed consent was exempted by the IRB. Each patient in the study received no other treatment prior to surgery, and *Table 1* lists the clinical sample features. For evaluating MIR4435-2HG clinical significance, this study assigned the PC samples into high- (n=34) and low-expression (n=26) groups according to the MIR4435-2HG median expression. Moreover, our study adhered to the 8th American Joint Committee on Cancer (AJCC) staging system to define the tumor/node/metastasis (TNM) stage (19). Post-operative samples were instantly immersed in liquid nitrogen and kept at –80 ℃ for subsequent analyses.

Cell culture and transfection

The human PC cell lines (PANC-1, BxPC-3, SW1990, and AsPC1) acquired from the Shanghai Institute of Biochemistry and Cellular Biology (Shanghai, China) and the human pancreatic normal ductal epithelial cell HPDE acquired from the BeNa Culture Collection (Beijing, China) were cultured using Roswell Park Memorial Institute (RPMI) 1640 medium (Gibco, China) or Dulbecco's modified Eagle's medium (DMEM, VivaCell, China) which contain 10% fetal bovine serum (FBS, ABW, Germany) and 1% penicillin/streptomycin (BasalMedia, China). The culture was maintained at 37 ℃ in a 5% CO_2 incubator.

Generating short hairpin RNAs (shRNAs) for MIR4435-2HG (sh-MIR4435-2HG#1/2) knockdown as well as negative control (sh-NC) was conducted through GeneCarer (Xi'an). The construction of MiR-128-3p mimics/NC mimics and miR-128-3p inhibitor/NC inhibitors was performed by GenePharma (Shanghai). Moreover, transfection was conducted employing PEI 40 K Transfection (Servicebio, China) per the protocols. Following a 48-h period of transfection, the transfection impact was assessed using qRT-PCR.

qRT-PCR analysis

Total RNA was extracted through a Trizol reagent (TaKaRa) while using the PrimeScript RTTM RT reagent Kit with gDNA Eraser (Takara) for complementary DNA (cDNA) quantification and synthesis. The qRT-PCR was conducted utilizing the SYBR® Premix ExTaq kit (TaKaRa) on the ABI7500 apparatus (BIO-RAD, Singapore). This study performed the $2^{-\Delta\Delta Cq}$ method for determining the tested gene relative expression levels. *Table 2* summarizes the primer sequences used.

Additionally, we deployed glyceraldehyde-3-phosphate dehydrogenase (GAPDH) as an internal control for MIR4435-2HG and ABHD17C while normalizing

Table 2 The primer sequences utilized

Primer	Sequence	
	Forward	Reverse
MIR4435-2HG	5'-GACTCTCCTACTGGTGCTTGGT-3'	5'-CACTGCCTGGTGAGCCTGTT-3'
miR-128-3p	5'-TGCGGCAGTGGTTTTACCCTATG-3'	5'-CCAGTGCAGGGTCCGAGGT-3'
ABHD17C	5'-GTCAGAGCATTGGGACTG-3'	5'-GATATCTTGTCAATGCTGGG-3'
GAPDH	5'-AAGGTGAAGGTCGGAGTCAAC-3'	5'-GGGGTCATTGATGGCAACAATA-3'
U6	5'-CTCGCTTCGGCAGCACA-3'	5'-AACGCTTCACGAATTTGCGT-3'

miR-128-3p relative expression using U6.

Cell Counting Kit 8 (CCK-8) assay

The study utilized CCK-8 Kit (Beyotime, Shanghai, China) to detect cell proliferation per the protocols. The cells (2,000 cells/well) were seeded and incubated in 96-well plates, and CCK-8 reagents were added into each well at 10, 24, 48, and 72 h, followed by incubation in an incubator at 37 ℃ with 5% CO_2 for 2 hours. The study utilized a microplate reader to assess the cell viability at 450 nm.

Transwell assay

The study performed the migration assay within 24-well transwell chambers (Corning Incorporated, USA). The culture of the transfected cells was conducted in the upper chambers in the absence of Matrigel (Millipore). Subsequently, 700 µL of a medium that contained 20% FBS was introduced to the lower chambers and followed by 24 h incubation. Then, lower chamber surface-transferred PC cells were fixed utilizing 4% paraformaldehyde and stained utilizing 0.1% crystal violet. Furthermore, the cells that had undergone migration were detected through a microscope (Olympus, Tokyo, Japan). The same method was repeated to conduct matrix-coated transwell invasion experiments in the upper chamber.

Wound healing assay

PC cells PANC-1 and SW1990 were seeded into six-well plates and cultured in DMEM or RPMI 1640 medium until reaching 100% confluence. The cell monolayer was scratched using a 200-µL pipette tip, followed by two washes with PBS and addition of serum-free medium. Wound healing process was observed under a microscope (Olympus, Tokyo, Japan) at 0 and 24 h.

RNA binding protein immunoprecipitation (RIP) assay

Herein, we employed a RIP assay kit (Genecreate, China) to assess its binding to Ago2. PC cells PANC-1 and SW1990 were rinsed utilizing cold PBS and lysed using 400 µL complete RIP lysis buffer for 30 min on ice. To obtain the supernatant, the cell lysate went through 10 min centrifugation at 12,000 rpm at 4 ℃. Next, 30 µL of protein A/G magnetic beads went through resuspension in 100 µL of RIP wash buffer and incubation with 5 µg of Ago2 antibody (1:50, Abcam) or IgG antibody (1:100, Abcam) for 30-min period. The antibody-bead complex was mixed with 900 µL and 150 of RIP immunoprecipitation buffer and cell supernatant, respectively, which was followed by overnight incubation at 4 ℃. A magnetic rack was employed for the collection of the beads-antibody-antigen complexes. Finally, the RNA was extracted to conduct a qRT-PCR analysis.

RNA pull-down assay

According to the protocol provided by the RNA pull-down assay kit (Genecreate, China), PC cells PANC-1 and SW1990 were harvested. Subsequently, the cell pellets were lysed on ice for 30 minutes using 500 µL of IP lysis buffer, followed by 4 minutes of sonication. The cell lysates were then centrifuged at 12,000 rpm and 4 ℃ for 10 minutes to obtain the supernatant. The 5' biotinylated miR-128-3p pull-down probe or the NC pull-down probe was incubated with the PC cells PANC-1 or SW1990 lysate at 4 ℃ with gentle agitation for 2 h. Subsequently, protein/RNA-RNA-magnetic beads were collected using a magnetic stand. Finally, RNA was extracted for qRT-PCR analysis.

Dual-luciferase reporter (DLR) assay

MIR4435-2HG wild (WT-MIR4435-2HG) and mutant (MUT-MIR4435-2HG) types, which either contained or lacked the miR-128-3p interacting site, were subjected to co-transfection into HEK293T cells and miR-NC or miR-128-3p mimics through Lipofectamine 3000 (Invitrogen). Our study utilized a luciferase reporter system (Promega Corporation) for assessing luciferase activity 48 h post-transfection.

Flow cytometry assay

Annexin V-IF647/PI Cell Apoptosis Detection Kit (Servicebio, Wuhan, China) was employed to determine the cell apoptosis ratio. PC cells PANC-1 and SW1990 in the exponential phase were collected and subjected to two washes with PBS, followed by resuspending 5×10^5 cells in 1 mL of binding buffer. After that, a 100-mL sample of the cell suspension went through 10 min incubation alongside propidium iodide (PI) and Annexin V-IF64 in darkness. Eventually, we deployed an Advanteon flow cytometer (Agilent, USA) for measuring the apoptotic ratio.

Western blot assay

The study employed not only a radioimmunoprecipitation assay (RIPA) kit (Boster, China) to extract total protein from cells but also a bicinchoninic acid (BCA) kit (Boster, China) for evaluating protein concentration. After electrophoresis on polyacrylamide gels, the protein was transferred to membranes (0.45 μm, Servicebio). The membrane was then maintained for 1 h in 5% skimmed milk and followed by overnight incubation at 4 ℃ with the specified rabbit antibodies (1:1,000, Thermo Fisher Scientific) and ABHD17C (1:1,000, Thermo Fisher Scientific). As an internal control, β-actin (1:1,000, Servicebio) was utilized. The membranes went through incubation with the secondary antibody for 1 h at 37 ℃. Detecting visible protein levels was conducted through enhanced chemiluminescence using the ECL assay (Servicebio, China).

Animal experiment

Experiments were performed under a project license (No. LDYYLL2022-505) granted by the ethics board of The First Hospital of Lanzhou University, in compliance with The First Hospital of Lanzhou University guidelines for the care and use of animals. The 6-week-old nude mice were subcutaneously injected with PC cells PANC-1 (2×10^6) transfected with either sh-MIR4435-2HG or sh-NC. Tumor volume and weight were examined at regular intervals of four days throughout seven instances. Mice were then euthanized, and tumor volumes and weights were measured. Tumor tissues were fractionated for immunohistochemistry (IHC) and haematoxylin and eosin (H&E), partially kept at –80 ℃, and RNA was extracted.

IHC staining

Paraffin-embedded tumor tissues were baked at 65 ℃ for 90 min to remove paraffin, followed by sequential immersion in xylene and ethanol solvents. After deparaffinization, the sections were hydrated in different concentrations of ethanol and distilled water. Subsequently, they were immersed in a repair solution and underwent high and low temperature treatment before cooling to room temperature for repair. Afterward, the sections were washed with tris-buffered saline tween (TBST), coated with blocking solution, and washed again with TBST. Normal goat serum was then applied to block the tissue. Finally, the sections were incubated overnight at 4 ℃ with the primary antibody against Ki67 (Proteintech), followed by incubation with the secondary antibody and subsequent IHC analysis.

Statistical analysis

The study utilized SPSS 25.0 (IBM Corp., Armonk, NY, USA) and GraphPad Prism 8.0 (GraphPad Software, San Diego, CA, USA) for conducting the statistical analyses, reporting the data as mean ± standard deviation (SD). Students' *t*-tests or one-way ANOVA were deployed for statistical differences. This study employed Spearman correlation analysis to detect correlations between MIR4435-2HG, miR-128-3p, and ABHD17C levels. $P<0.05$ indicated statistical significance.

Results

MIR4435-2HG is overexpressed in PC tissues and cells

PC tissues showed higher MIR4435-2HG expression than normal pancreatic tissues (*Figure 1A*). Moreover, patients with PC overexpressing MIR4435-2HG had poor prognoses (*Figure 1B-1D*). The prognosis of patients with PC is influenced by independent risk factors such as MIR4435-2HG and N stage, as demonstrated via univariate

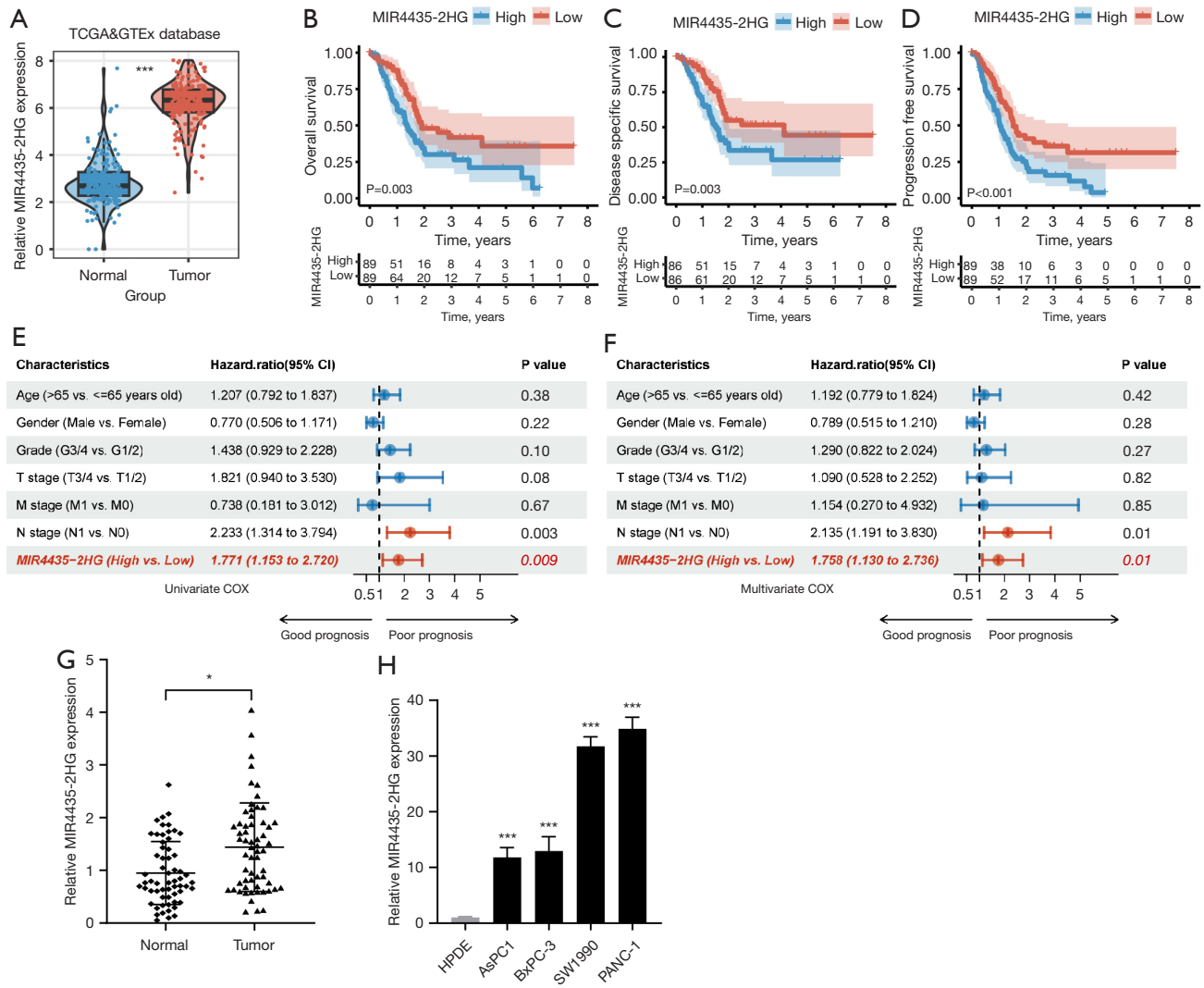

Figure 1 MIR4435 overexpression in pancreatic cancer tissues and cell lines. (A) PC tissues exhibiting a higher MIR4435-2HG expression than normal pancreatic tissues. (B-D) Pancreatic cancer patients having higher MIR4435-2HG expression show a worse prognosis. (E,F) Univariate and multivariate Cox regression analyses demonstrating MIR4435-2HG and N stage as independent risk factors for prognosis in pancreatic cancer patients. (G) Detecting MIR4435-2HG expression in 60 pairs of pancreatic cancer and paired normal pancreas samples employing quantitative real-time polymerase chain reaction. (H) Basal expression of MIR4435-2HG in HPDE, AsPC1, BxPC-3, SW1990, and PANC-1 cells. *, P<0.05; ***, P<0.001. TCGA, The Cancer Genome Atlas; GTEx, Genotype-Tissue Expression; TNM, tumor/node/metastasis; CI, confidence interval; PC, pancreatic cancer.

and multivariate Cox regression analyses (*Figure 1E,1F*). MIR4435-2HG exhibited significant overexpression in PC tissues compared with normal tissues (*Figure 1G*). Compared to the human pancreatic normal ductal epithelial cell HPDE, MIR4435-2HG was found to exhibit significant overexpression in the four PC cell lines, while PC cells PANC-1 and SW1990 exhibited significant MIR4435-2HG overexpression (*Figure 1H*). These results indicate that MIR4435-2HG could be a PC prognostic biomarker.

Knocking down MIR4435-2HG suppresses PC cell malignant behavior and promotes apoptosis

This study employed shRNA (sh-MIR4435-2HG#1/2) to suppress MIR4435-2HG expression in PC cells PANC-1 and SW1990 for investigating the biological function of

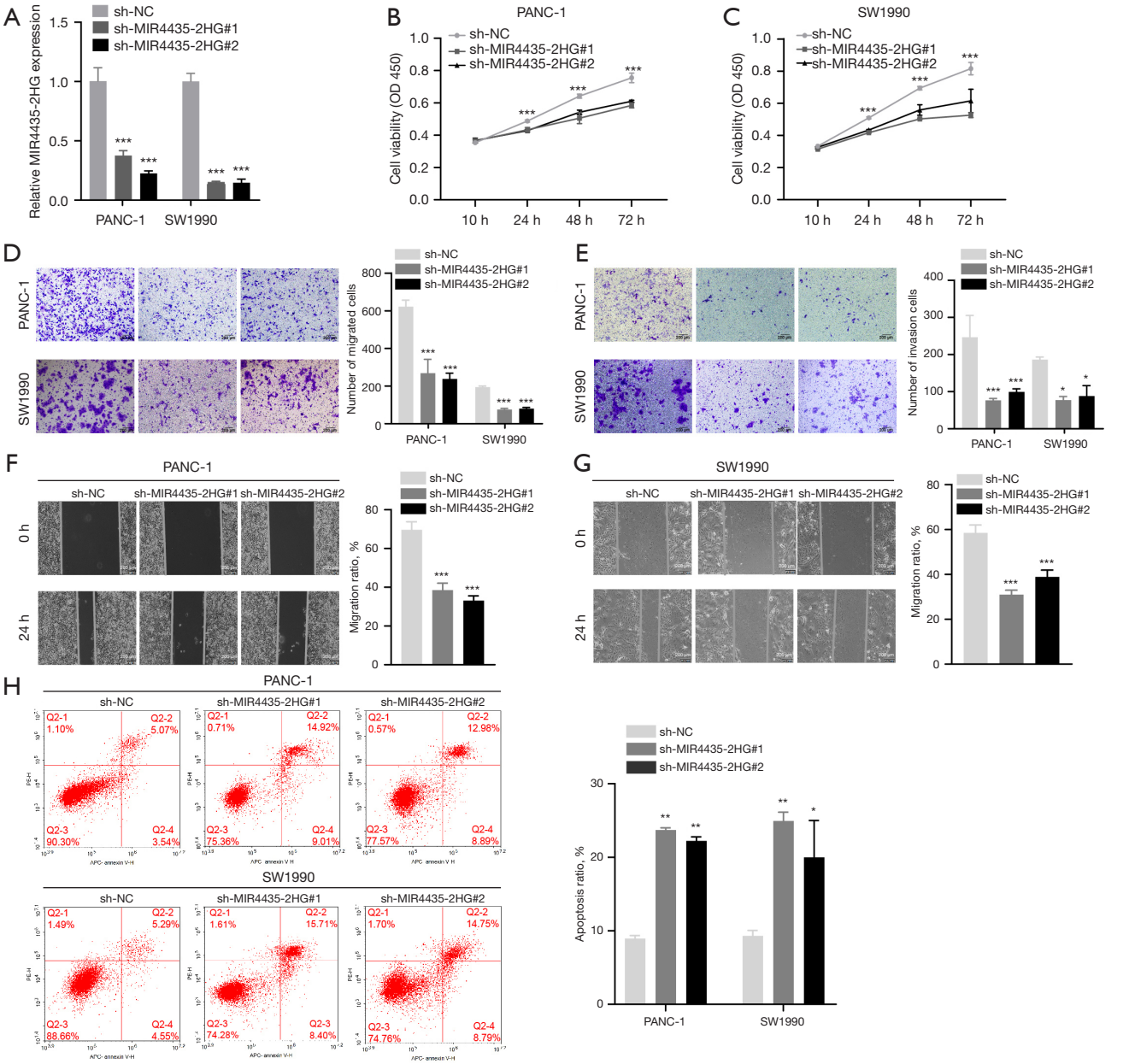

Figure 2 MIR4435-2HG knocking down suppressed pancreatic cancer cell progression. (A) Validation of MIR4435-2HG knockdown efficiency through quantitative real-time polymerase chain reaction. (B,C) CCK-8 assay for assessing proliferation of MIR4435-2HG knockdown pancreatic cancer cells PANC-1 and SW1990 *in vitro*. (D,E) Transwell assay (without/with Matrigel) for PANC-1 and SW1990 cell ability to migrate and invade following MIR4435-2HG knockdown (crystal violet stain). (F,G) MIR4435-2HG knockdown of PANC-1 and SW1990 migration ratio observed through wound healing assays (10×). (H) Flow cytometry detecting PANC-1 and SW1990 cell apoptosis following knocking down MIR4435-2HG. *, P<0.05; **, P<0.01; ***, P<0.001. NC, negative control; OD, optical density; CCK-8, Cell Counting Kit 8.

MIR4435-2HG in PC cells (*Figure 2A*). CCK-8 assay results depicted that sh-MIR4435-2HG#1/2 significantly reduced the cell proliferation of PC cells PANC-1 and SW1990 (*Figure 2B,2C*). The transwell assay without Matrigel demonstrated that sh-MIR4435-2HG#1/2 effectively inhibited the migration of PC cells PANC-1 and

SW1990 (*Figure 2D*). Similarly, the transwell assay with Matrigel depicted reduced invasive capabilities of PC cells (*Figure 2E*). Wound healing assays illustrated a notable decrease in sh-MIR4435-2HG#1/2 PC cell migration rate (*Figure 2F,2G*). The flow cytometry analysis indicated that sh-MIR4435-2HG#1/2 can induce apoptosis in PC cells (*Figure 2H*). Collectively, these findings suggest that knockdown of MIR4435-2HG promotes apoptosis, underscoring its probability as a tumor suppressor in PC development.

MIR4435-2HG negatively regulates miR-128-3p

Bioinformatics databases (starBase v3.0 and RNAInter) were employed to predict miRNAs that MIR4435-2HG could potentially sponge, resulting in identifying miR-128-3p through the intersection (*Figure 3A*). PC patients with downregulated miR-128-3p exhibited a poorer prognosis (*Figure 3B*). MIR4435-2HG exhibited a negative correlation with miR-128-3p (*Figure 3C*); therefore, it was selected for subsequent analyses. The study employed qRT-PCR to examine miR-128-3p expression in HPDE, PANC-1, and SW1990 cell lines and in 60 pairs of PC samples and normal tissues, revealing that miR-128-3p exhibited a significant reduction in PC cell PANC-1 and SW1990 than the human pancreatic normal ductal epithelial cell HPDE (*Figure 3D*), miR-128-3p was downregulated in PC tissues (*Figure 3E*). In addition, miR-128-3p mimics resulted in MIR4435-2HG suppression, while miR-128-3p inhibitor intervention presented the opposite result in PC cell PANC-1 and SW1990 (*Figure 3F,3G*). *Figure 3H* illustrates the miR-128-3p binding sequence to MIR4435-2HG. In addition, DLR assay results depicted that higher miR-128-3p expression significantly hindered MIR4435-2HG-WT luciferase activity without affecting MIR4435-2HG-Mut (*Figure 3I*). The results of the RNA pull-down assay showed that MIR4435-2HG was specifically enriched in the miR-128-3p probe group compared to the control probe (*Figure 3J,3K*). Depending on RIP analysis results, the Ago2 antibody was highly enriched for MIR4435-2HG as well as miR-128-3p in PC cells PANC-1 and SW1990, while IgG antibody barely detected them (*Figure 3L,3M*). Moreover, a significant inverse correlation existed between miR-128-3p and MIR4435-2HG expressions in PC tissues (R^2=0.1635, P=0.001; *Figure 3N*). This evidence signifies the role of MIR4435-2HG as a miRNA sponge and its negative regulation for miR-128-3p expression.

ABHD17C is a miR-128-3p target gene

Herein, we accessed bioinformatics databases (starBase v3.0, miRDB, and miRTarBase) to predict miR-128-3p target genes. The intersection of these predictions with genes from TCGA exhibiting $\log_2$ fold change (FC) >1 and poor prognosis yielded four potential target genes (*Figure 4A,4B*). The qRT-PCR further validated the significant upregulation of ABHD17C expression in PC cell PANC-1 and SW1990 than the human pancreatic normal ductal epithelial cell HPDE (*Figure 4C*). Therefore, ABHD17C was selected for further analysis. PC patients with overexpressed ABHD17C had poor prognoses (*Figure 4D-4F*), and ABHD17C exhibited a negative correlation with miR-128-3p (*Figure 4G*). The qRT-PCR results in detecting ABHD17C expression within 60 pairs of PC and adjacent normal tissue samples revealed that ABHD17C was overexpressed in PC tissues (*Figure 4H*). MiR-128-3p mimics caused ABHD17C suppression, while miR-128-3p inhibitor intervention presented the opposite result (*Figure 4I,4J*). *Figure 4K* illustrates the miR-128-3p binding sequence in ABHD17C. Based on DLR assay results, miR-128-3p overexpression significantly hindered ABHD17C-WT LUS activity but had no influence on ABHD17C-Mut (*Figure 4L*). The results of the RNA pull-down assay showed that ABHD17C was specifically enriched in the miR-128-3p probe group compared to the control probe (*Figure 4M,4N*). RIP analysis results illustrated that the Ago2 antibody was enriched for miR-128-3p and ABHD17C in PC cell PANC-1 and SW1990, whereas the IgG antibody barely detected miR-128-3p and ABHD17C (*Figure 4O,4P*). Additionally, ABHD17C expression in PC tissues was revealed to exhibit a negative correlation with miR-128-3p expression (R^2=0.1789, P<0.001; *Figure 4Q*). This evidence suggests that ABHD17C is an miR-128-3p target.

MIR4435-2HG positively regulates PC progression via modulating the miR-128-3p/ABHD17C

To validate the contribution of MIR4435-2HG to promoting PC progression via the miR-128-3p/ABHD17C pathway, we intervened PC cells PANC-1 and SW1990 employing miR-128-3p inhibitor to examine ABHD17C expression and the cellular malignant phenotype. qRT-PCR analysis revealed significant inhibition of ABHD17C in the sh-MIR4435-2HG#1 group compared to the sh-NC group. Additionally, ABHD17C was significantly

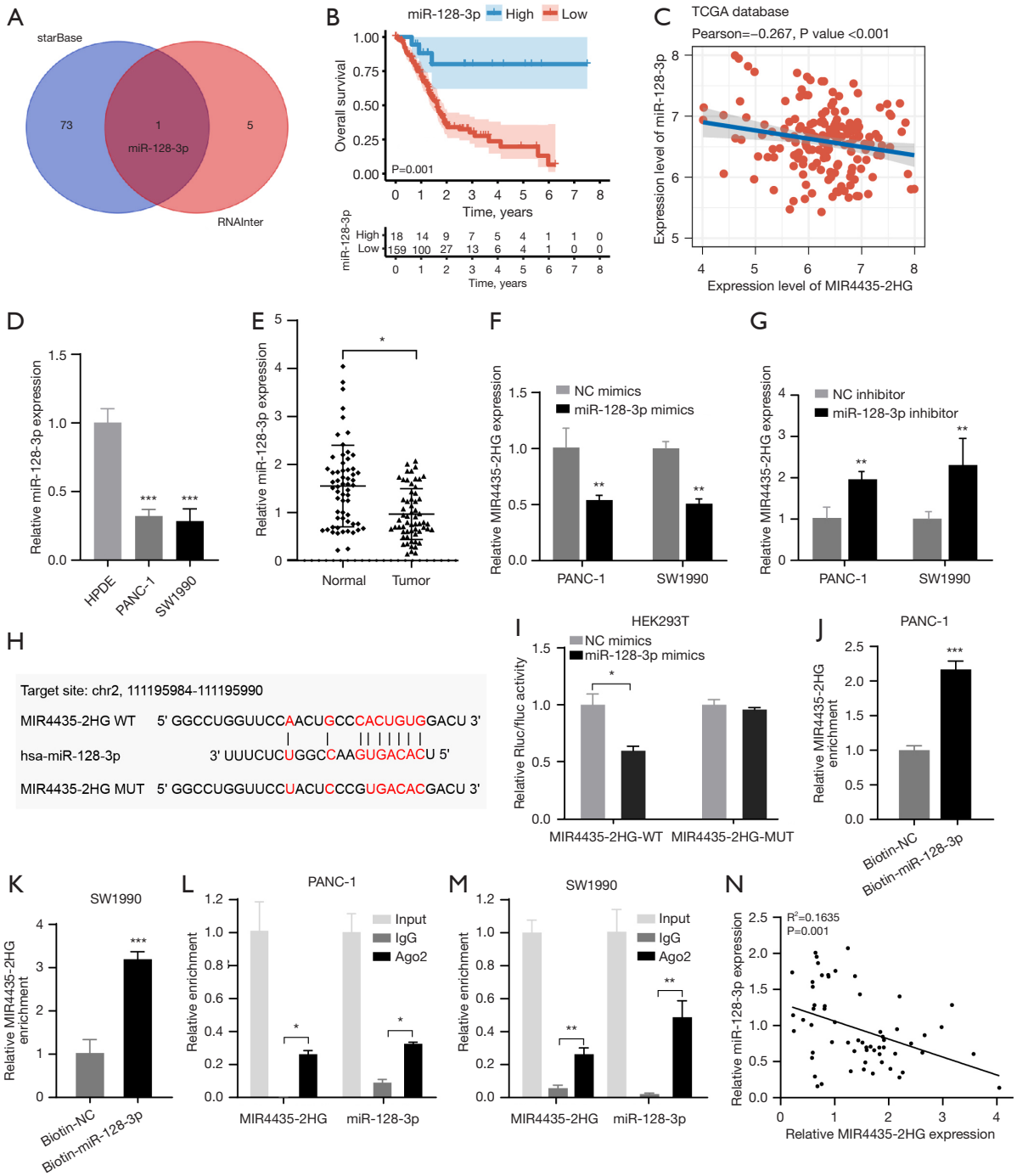

Figure 3 MIR4435-2HG serves as an miR-128-3p sponge. (A) RNAInter and starBase predicting the miRNAs that MIR4435-2HG might potentially sponge. (B) Pancreatic cancer patients having a downregulated miR-128-3p exhibit a worse prognosis. (C) MIR4435-2HG negative correlation with miR-128-3p expression. (D) Determining miR-128-3p expression in HPDE, PANC-1, and SW1990 cells through quantitative real-time polymerase chain reaction. (E) Detecting miR-128-3p expression within 60 pairs of pancreatic cancer and paired normal pancreas specimens using quantitative real-time polymerase chain reaction. (F,G) Determining the impact of miR-128-3p mimics and inhibitors on MIR4435-2HG expression in PANC-1 and SW1990 cells via quantitative real-time polymerase chain reaction. (H) Sequence of miR-128-3p with the MIR4435-2HG binding site. (I) Validation of miR-128-3p association with MIR4435-2HG via dual-luciferase reporter assay. (J,K) Detecting MIR4435-2HG binding to miR-128-3p through RNA pull-down assay. (L,M) Detecting MIR4435-2HG binding to miR-128-3p through RIP assay. (N) Analyzing MIR4435-2HG correlation with miR-128-3p expression within pancreatic cancer tissues employing Spearman's correlation analysis. *, P<0.05; **, P<0.01; ***, P<0.001. TCGA, The Cancer Genome Atlas; NC, negative control; WT, wild-type; MUT, mutation; ; RIP, RNA binding protein immunoprecipitation.

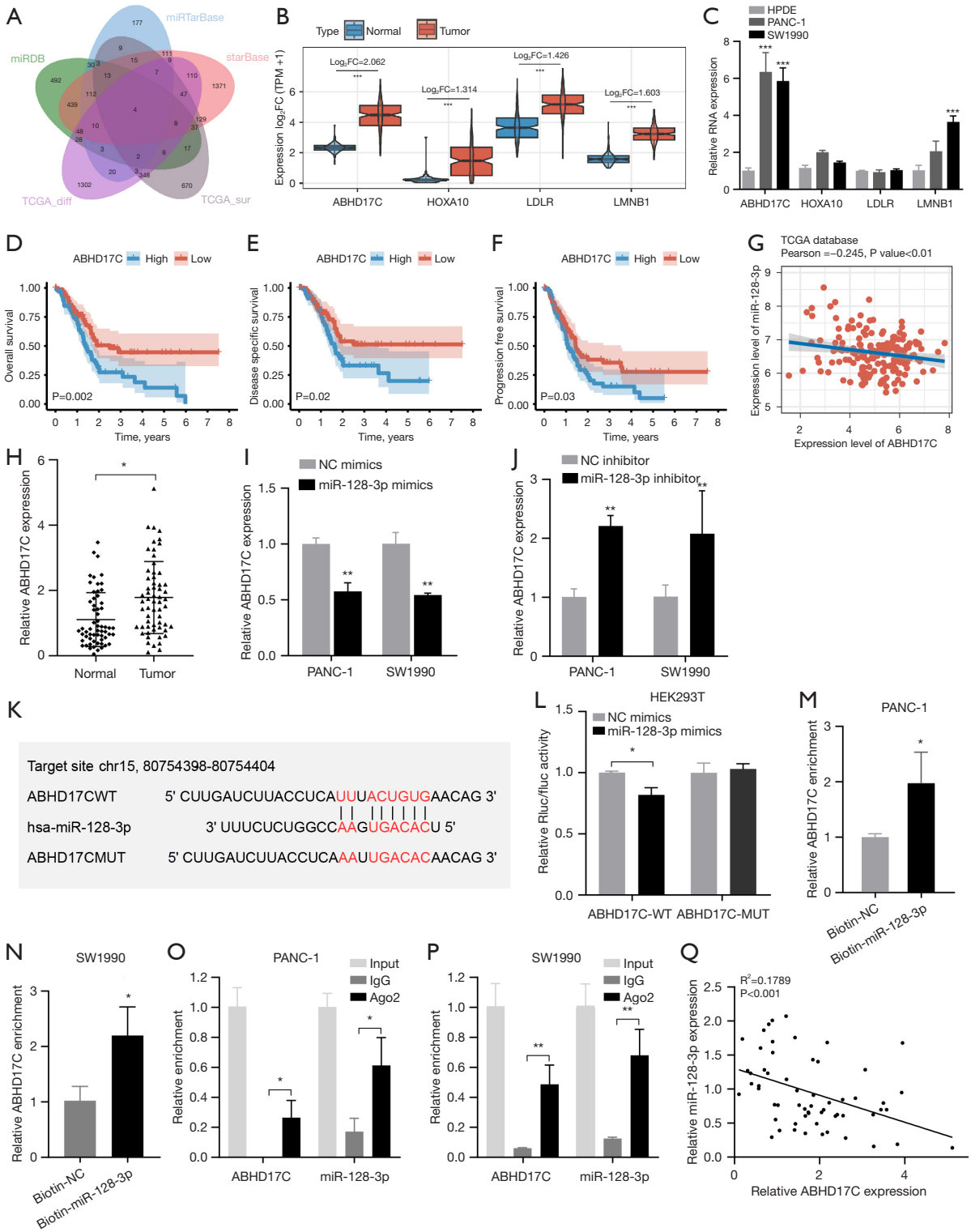

Figure 4 ABHD17C represents a miR-128-3p target. (A) Bioinformatics databases predict miR-128-3p target genes. (B) The four miR-128-3p target gene expression obtained by interaction. (C) Determining the four miR-128-3p target gene expression within HPDE, PANC-1, and SW1990 cells through quantitative real-time polymerase chain reaction. (D-F) Pancreatic cancer patients with higher ABHD17C expression have a worse prognosis. (G) The negative correlation of ABHD17C with miR-128-3p expression. (H) Detection of ABHD17C

expression in 60 pairs of pancreatic cancer specimens and paired normal pancreas specimens using quantitative real-time polymerase chain reaction. (I,J) Examining the influence of miR-128-3p mimics and inhibitors on ABHD17C expression in pancreatic cancer cells PANC-1 and SW1990 employing quantitative real-time polymerase chain reaction. (K) Sequence of miR-128-3p with ABHD17C binding site. (L) Validation of miR-128-3p relation to ABHD17C employing dual-luciferase reporter assay. (M,N) Detecting miR-128-3p binding to ABHD17C by RNA pull-down assay. (O,P) Detecting miR-128-3p binding to ABHD17C by RIP assay. (Q) Analyzing miR-128-3p correlation with ABHD17C expression in pancreatic cancer tissues via Spearman's correlation analysis. *, P<0.05; **, P<0.01; ***, P<0.001. TCGA, The Cancer Genome Atlas; FC, fold change; TPM, transcript per million; WT, wild-type; MUT, mutation; RIP, RNA binding protein immunoprecipitation.

overexpressed upon introducing miR-128-3p inhibitor (*Figure 5A*). Further, ABHD17C expression had a positive correlation in PC tissues with that of MIR4435-2HG (R^2=0.3046, P<0.001; *Figure 5B*). CCK-8 results disclosed that MIR4435-2HG knockdown had a suppressive effect on cell proliferation of PC cells PANC-1 and SW1990. Conversely, the inhibitory effect of sh-MIR4435-2HG#1 was reverted by adding miR-128-3p inhibitor (*Figure 5C,5D*). Transwell (without Matrigel) displayed that MIR4435-2HG knockdown significantly reduced the cell migration of PC cells PANC-1 and SW1990, which was reversed upon adding miR-128-3p inhibitor (*Figure 5E*). Transwell (with Matrigel) indicated that MIR4435-2HG knockdown caused a significant inhibition of the cell invasion of PC cells PANC-1 and SW1990. Conversely, the miR-128-3p inhibitor enhanced the invasion ability (*Figure 5F*). The wound healing assay results demonstrated that knocking down MIR4435-2HG inhibited the cell migration rates of PC cells PANC-1 and SW1990, while miR-128-3p inhibitors promoted migratory capacity (*Figure 6A*). The results of flow cytometry represented that apoptosis induction was enhanced in sh-MIR4435-2HG#1-transfected PC cells PANC-1 and SW1990. Conversely, the miR-128-3p inhibitor resulted in a reduction in apoptosis (*Figure 6B*). These results confirm that MIR4435-2HG participates in PC progression by targeting the miR-128-3p/ABHD17C axis.

Knocking down of MIR4435-2HG suppresses PC tumorigenesis in vivo

To determine MIR4435-2HG function *in vivo*, we subcutaneously injected sh-MIR4435-2HG#1 PANC-1 cells into the mice. The sh-MIR4435-2HG#1 tumor volumes and weights were significantly lower than those of sh-NC (*Figure 7A-7C*). Meanwhile, we observed a sh-MIR4435-2HG#1 group MIR4435-2HG downregulation (*Figure 7D*), a miR-128-3p overexpression (*Figure 7E*), and an ABHD17C mRNA and protein level suppression (*Figure 7F,7G*). The results of H&E staining revealed that the tumor cells in the sh-NC group had larger nuclei, stained more deeply, and presented significantly different cellular morphology characteristics from the sh-MIR4435-2HG#1 group, and the results of IHC staining for the cell proliferation marker Ki67 showed a decreased proportion of Ki67-positive tumor cells in the sh-MIR4435-2HG#1 group in comparison to the sh-NC group (*Figure 7H*). Collectively, MIR4435-2HG promotes tumor growth by overexpressing ABHD17C and reducing miR-128-3p *in vivo*.

Discussion

Currently, lncRNAs have emerged as significant players in tumor progression. They often act as oncogenes, driving cell proliferation, invasion, and metastasis, and even contribute to drug resistance in various cancers (20,21). Among these, MIR4435-2HG, a newly discovered lncRNA, has gained attention due to its elevated expression and involvement in cancer progression. MIR4435-2HG has a close relation to clinicopathological features and poor prognosis in several malignancies, making it a valuable diagnostic and prognostic marker for cancer (11,22,23). Nevertheless, the precise function of MIR4435-2HG in PC progression is still unknown. Accordingly, our aim was to elucidate the precise MIR4435-2HG contribution to PC development. The qRT-PCR results revealed significant MIR4435-2HG overexpression in PC tissues and cell lines. Subsequent *in vitro* experiments demonstrated that MIR4435-2HG knockdown substantially reduced PANC-1 and SW1990 cell ability to proliferate, migrate, and invade, accompanied by apoptosis induction. Collectively, MIR4435-2HG is pivotal in promoting PC progression. Additionally, our results suggest that MIR4435-2HG has independent prognostic value for OS in PC patients. MIR4435-2HG has been considered a promising biomarker for HCC diagnosis and prognosis (24) and to

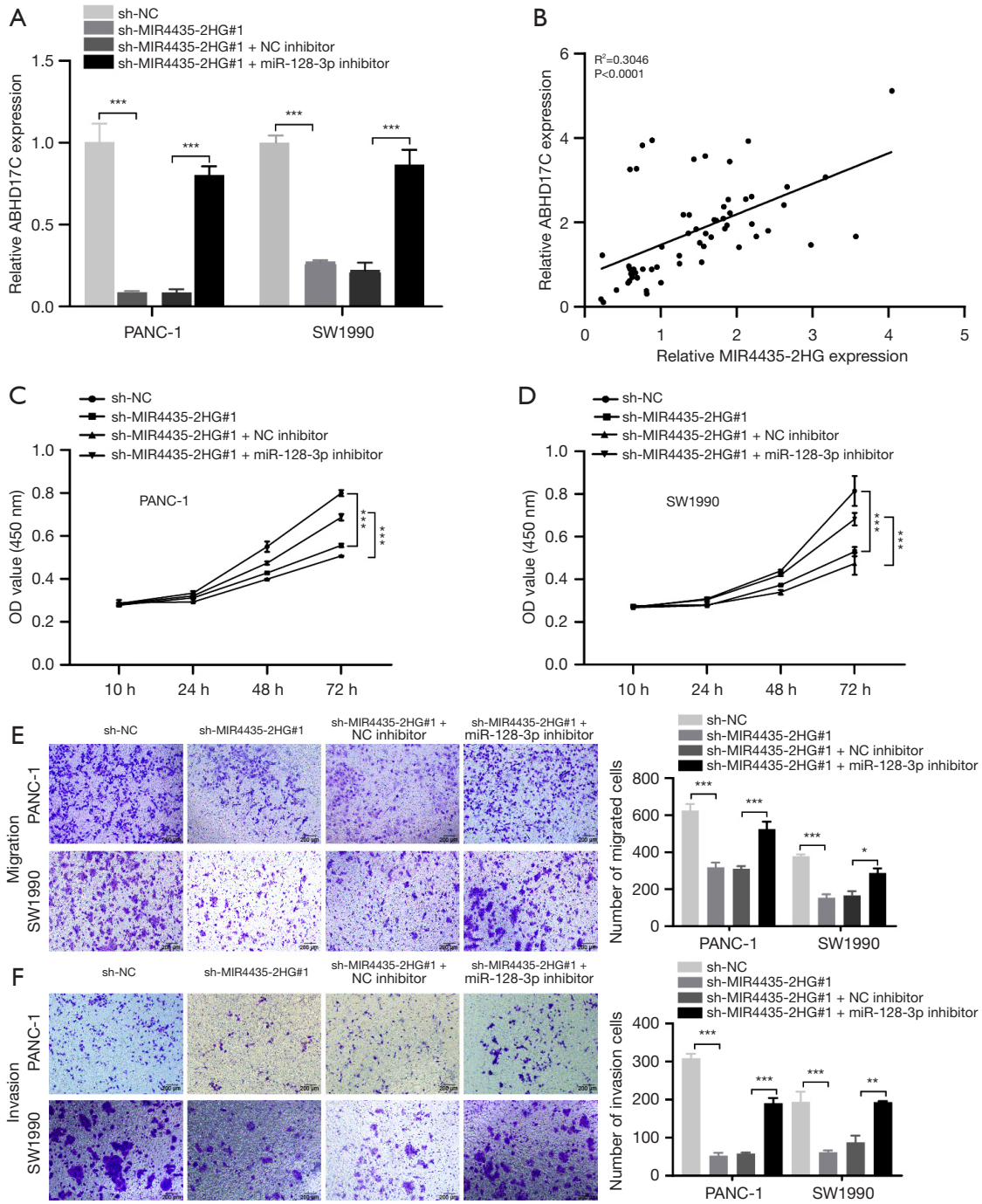

Figure 5 MiR-128-3p inhibitor reversing the impact of knocking down MIR4435-2HG on pancreatic cancer cell progression. (A) Measuring ABHD17C mRNA levels in PANC-1 and SW1990 cells transfected with sh-NC, sh-MIR4435-2HG#1, sh-MIR4435-2HG#1 + NC inhibitor or sh-MIR4435-2HG#1 + miR-128-3p inhibitor through quantitative real-time polymerase chain reaction. (B) Analyzing MIR4435-2HG correlation with ABHD17C expression in pancreatic cancer tissues via Spearman's correlation analysis. (C,D) Detecting cell proliferation with CCK-8 assay. (E,F) Determining PANC-1 and SW1990 cell migration and invasion via transwell assay (without/with Matrigel, crystal violet stain). *, P<0.05; **, P<0.01; ***, P<0.001. NC, negative control; OD, optical density; CCK-8, Cell Counting Kit 8.

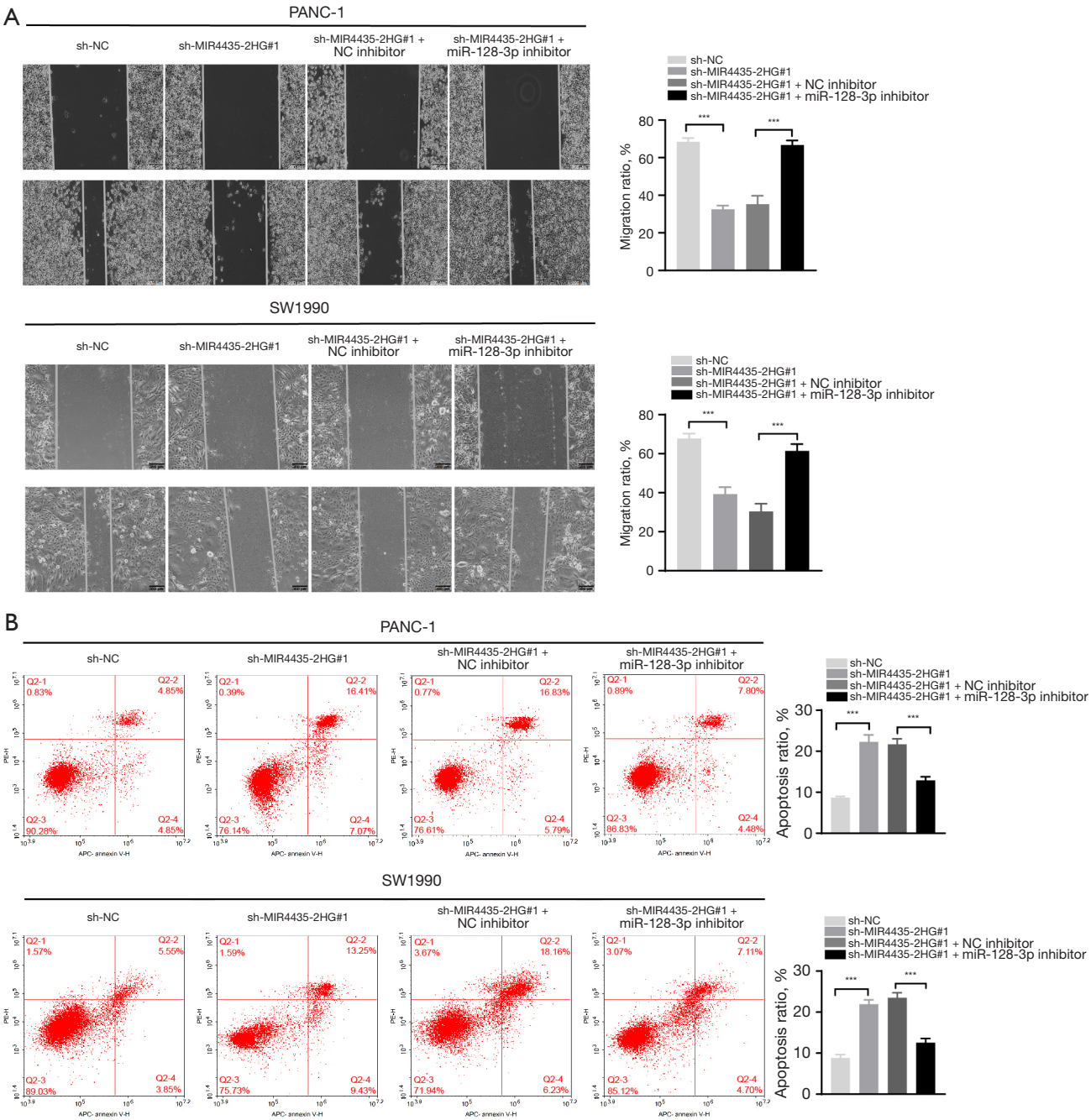

Figure 6 MiR-128-3p inhibitor reversing the impact of knocking down MIR4435-2HG on pancreatic cancer cell apoptosis and migration by upregulating ABHD17C. (A) Observing the cell migration ratio through wound healing assays (10×). (B) Determining the PANC-1 and SW1990 cell apoptosis ratio with flow cytometry. ***, P<0.001. NC, negative control.

enhance the proliferative and invasive abilities of lung and gastric cancer cells *in vitro* and *in vivo* via activating the β-catenin signaling pathway (25,26). Prior research has demonstrated that MIR4435-2HG silencing inhibits HNSCC, prostate cancer, and non-small cell lung cancer cell migration and invasion (10,27,28), which is consistent with our results. While lncRNAs, including MIR4435-2HG, can be excellent biomarkers for diagnosing and

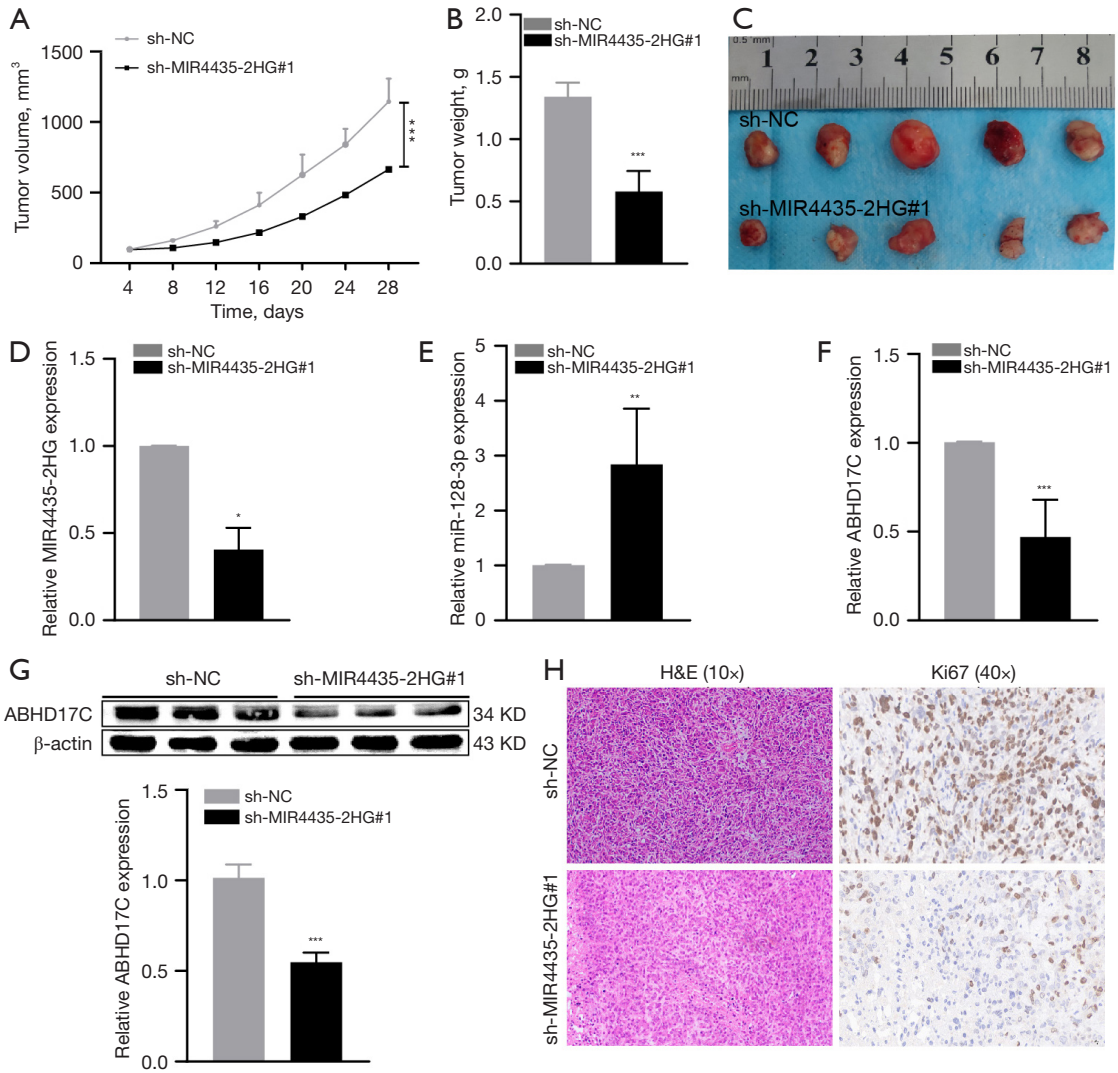

Figure 7 Tumor growth suppression *in vivo* by knocking down MIR4435-2HG. Injecting the nude mice with PANC-1 cells that were transfected with either sh-MIR4435-2HG#1 or sh-NC. (A) Performing tumor volume calculations at four-day intervals. (B) The resected tumor tissue weight and (C) size. (D-F) MIR4435-2HG, miR-128-3p, and ABHD17C expressions in excised tumor tissues. (G) Determining ABHD17C protein levels excised tumor tissues using Western blot. (H) Illustration of hematoxylin & eosin staining (10×) and immunohistochemical staining (40×) using the Ki67 antibody. *, P<0.05; **, P<0.01; ***, P<0.001. NC, negative control.

assessing the prognosis of PC, and can serve as reliable supplements to traditional PC tests, their vast potential in PC diagnosis and treatment still requires exploration (29). Ensuring the specificity and sensitivity of lncRNA-based approaches is essential due to lncRNAs' tissue-specific expression patterns and subtle dysregulation. Developing precise detection methods is crucial for reliable clinical use. Additionally, clinical validation through large-scale trials is necessary to establish the utility of lncRNA-based diagnostics and therapies. This process involves defining robust biomarkers, determining optimal treatment strategies, and demonstrating efficacy and safety across diverse patient populations.

In various cancer types, lncRNAs serve as competing endogenous RNAs (ceRNAs), influencing miRNA target genes by acting as miRNA sponges (30-35). Specifically, MIR4435-2HG was found to enhance clear cell renal cell carcinoma and glioblastoma aggressiveness by governing target genes, namely KLF6 and TGFBR2, through miRNA sponging involving miR-513a-5p and miR-1224-5p,

respectively (33,36). The ceRNA role of MIR4435-2HG was also elucidated in HCC, breast, cervical, colorectal, and gastric cancers (14,37). This study encompasses a bioinformatics analysis on MIR4435-2HG-miR-128-3p interactions through online software, followed by validation of target binding through DLR assays. In gastric cancer, miR-128-3p expression is decreased, and when it is overexpressed, it inhibits proliferation and triggers apoptosis (38). miR-128-3p exhibits downregulation in patients with breast cancer within both blood and tissues (39,40). Its overexpression eliminates the stemness of breast cancer cells and reduces their migration from invasive breast cancer (17). These findings explain the probable significance of miR-128-3p in acting as a biomarker for transforming benign tumors into malignancies. Similar results have been observed for lung cancer (41), glioblastoma (42), and prostate cancer (43). The miR-128-3p has been revealed to exhibit significantly suppressed levels in PC tissues (44). MiR-128-3p functions as a tumor suppressor besides exerting regulatory effects on the proliferative and invading abilities of PC cells, which aligns with our results (45,46). Herein, we demonstrated a significantly downregulated miR-128-3p, which promotes PC cell ability to proliferate, migrate, and invade while inhibiting apoptosis, which aligns with prior research. This suggests the regulatory effect of MIR4435-2HG on miR-128-3p, contributing to PC progression.

ABHD17C refers to the α/β-hydrolase domain-containing protein 17C, also known to contain the α/β-hydrolase domain 17C. This protein belongs to the α/β-hydrolase enzyme family and serves as a novel protein, depalmitoylase, which is crucial in regulating protein localization and signaling (47,48). Research has revealed that ABHD17C is highly expressed in patient-derived tumor xenografts from breast tissue and breast cancer patients (49), making it a potential target for cabozantinib therapy in lung adenocarcinoma (50). Furthermore, an integrated analysis of multi-omics data has identified ABHD17C as a prognostic biomarker for PC (51). Herein, we revealed that miR-128-3p directly targeted ABHD17C in PC cells PANC-1 and SW1990. Moreover, our study provided evidence that MIR4435-2HG knockdown inhibits ABHD17C in PC cell lines. This effect was counteracted when a miR-128-3p inhibitor was co-transfected. MIR4435-2HG suppression reduced the proliferative, migrating, and invading abilities of the PC cell line while increasing apoptosis. The effects above were abolished through co-transfection with miR-128-3p inhibitor.

Conclusions

In conclusion, MIR4435-2HG is significantly upregulated in PC tissues compared to adjacent normal pancreatic tissues and is closely associated with poor patient prognosis. MIR4435-2HG plays an oncogenic role in PC by exerting positive regulation on the malignant biological behaviors of PC cells. Mechanistically, MIR4435-2HG competitively binds to miR-128-3p, reducing its expression levels, leading to increased expression of ABHD17C. Consequently, this promotes the proliferation, invasion, and migration of PC cells while simultaneously inhibiting apoptosis.

Acknowledgments

Funding: This work was supported by The First Hospital of Lanzhou University Intra-Hospital Fund Youth Fund (ldyyyn2022-38).

Footnote

Reporting Checklist: The authors have completed the MDAR and ARRIVE reporting checklists. Available at https://tcr.amegroups.com/article/view/10.21037/tcr-24-51/rc

Data Sharing Statement: Available at https://tcr.amegroups.com/article/view/10.21037/tcr-24-51/dss

Peer Review File: Available at https://tcr.amegroups.com/article/view/10.21037/tcr-24-51/prf

Conflicts of Interest: All authors have completed the ICMJE uniform disclosure form (available at https://tcr.amegroups.com/article/view/10.21037/tcr-24-51/coif). The authors have no conflicts of interest to declare.

Ethical Statement: The authors are accountable for all aspects of the work in ensuring that questions related to the accuracy or integrity of any part of the work are appropriately investigated and resolved. This study was conducted in accordance with the Declaration of Helsinki (as revised in 2013). This study including human sample and animal experimental protocols has been approved by its Institutional Review Board (IRB) of the First Hospital of Lanzhou University Ethics Committee (approval number: LDYYLL2022-505), in compliance with The First Hospital of Lanzhou University guidelines for the care and use of

animals. The informed consent was exempted by the IRB.

References

1. Rahib L, Smith BD, Aizenberg R, et al. Projecting cancer incidence and deaths to 2030: the unexpected burden of thyroid, liver, and pancreas cancers in the United States. Cancer Res 2014;74:2913-21.
2. Siegel RL, Miller KD, Jemal A. Cancer statistics, 2019. CA Cancer J Clin 2019;69:7-34.
3. Rustgi AK. Pancreatic cancer: novel approaches to diagnosis and therapy. Gastroenterology 2005;129:1344-7.
4. Makohon-Moore A, Iacobuzio-Donahue CA. Pancreatic cancer biology and genetics from an evolutionary perspective. Nat Rev Cancer 2016;16:553-65.
5. Han S, Chen X, Huang L. The tumor therapeutic potential of long non-coding RNA delivery and targeting. Acta Pharm Sin B 2023;13:1371-82.
6. Zong Y, Wang X, Cui B, et al. Decoding the regulatory roles of non-coding RNAs in cellular metabolism and disease. Mol Ther 2023;31:1562-76.
7. Shabna A, Bindhya S, Sidhanth C, et al. Long non-coding RNAs: Fundamental regulators and emerging targets of cancer stem cells. Biochim Biophys Acta Rev Cancer 2023;1878:188899.
8. Ye X, Wang LP, Han C, et al. Increased m(6)A modification of lncRNA DBH-AS1 suppresses pancreatic cancer growth and gemcitabine resistance via the miR-3163/USP44 axis. Ann Transl Med 2022;10:304.
9. Kotzin JJ, Spencer SP, McCright SJ, et al. The long non-coding RNA Morrbid regulates Bim and short-lived myeloid cell lifespan. Nature 2016;537:239-43.
10. Yang M, He X, Huang X, et al. LncRNA MIR4435-2HG-mediated upregulation of TGF-β1 promotes migration and proliferation of nonsmall cell lung cancer cells. Environ Toxicol 2020;35:582-90.
11. Ghasemian M, Rajabibazl M, Sahebi U, et al. Long non-coding RNA MIR4435-2HG: a key molecule in progression of cancer and non-cancerous disorders. Cancer Cell Int 2022;22:215.
12. Sheykhhasan M, Dermani FK, Gheibi N, et al. The emerging role of LncRNA AWPPH in multiple cancers: a review study. Curr Mol Med 2023. [Epub ahead of print]. doi: 10.2174/1566524023666230816163031.
13. Li S, Hu X, Yu S, et al. Hepatic stellate cell-released CXCL1 aggravates HCC malignant behaviors through the MIR4435-2HG/miR-506-3p/TGFB1 axis. Cancer Sci 2023;114:504-20.
14. Kong Q, Liang C, Jin Y, et al. The lncRNA MIR4435-2HG is upregulated in hepatocellular carcinoma and promotes cancer cell proliferation by upregulating miRNA-487a. Cell Mol Biol Lett 2019;24:26.
15. Cheng Z, Gong L, Cai Q. LncRNA00978 contributes to growth and metastasis of hepatocellular carcinoma cells via mediating microRNA-125b-5p/SOX12 pathway. Bioengineered 2022;13:11228-39.
16. Wang S, Chen X, Qiao T. Long non-coding RNA MIR4435-2HG promotes the progression of head and neck squamous cell carcinoma by regulating the miR-383-5p/RBM3 axis. Oncol Rep 2021;45:99.
17. Breunig C, Erdem N, Bott A, et al. TGFβ1 regulates HGF-induced cell migration and hepatocyte growth factor receptor MET expression via C-ets-1 and miR-128-3p in basal-like breast cancer. Mol Oncol 2018;12:1447-63.
18. Zhao J, Li D, Fang L. MiR-128-3p suppresses breast cancer cellular progression via targeting LIMK1. Biomed Pharmacother 2019;115:108947.
19. Nagaria TS, Wang H. Modification of the 8(th) AJCC staging system of pancreatic ductal adenocarcinoma. Hepatobiliary Surg Nutr 2020;9:95-7.
20. Sharma GG, Okada Y, Von Hoff D, et al. Non-coding RNA biomarkers in pancreatic ductal adenocarcinoma. Semin Cancer Biol 2021;75:153-68.
21. Xie W, Chu M, Song G, et al. Emerging roles of long noncoding RNAs in chemoresistance of pancreatic cancer. Semin Cancer Biol 2022;83:303-18.
22. Zhang M, Yu X, Zhang Q, et al. MIR4435-2HG: A newly proposed lncRNA in human cancer. Biomed Pharmacother 2022;150:112971.
23. Zhong C, Xie Z, Zeng LH, et al. MIR4435-2HG Is a Potential Pan-Cancer Biomarker for Diagnosis and Prognosis. Front Immunol 2022;13:855078.
24. Kunadirek P, Pinjaroen N, Nookaew I, et al. Transcriptomic Analyses Reveal Long Non-Coding

RNA in Peripheral Blood Mononuclear Cells as a Novel Biomarker for Diagnosis and Prognosis of Hepatocellular Carcinoma. Int J Mol Sci 2022;23:7882.
25. Qian H, Chen L, Huang J, et al. The lncRNA MIR4435-2HG promotes lung cancer progression by activating β-catenin signalling. J Mol Med (Berl) 2018;96:753-64.
26. Wang H, Wu M, Lu Y, et al. LncRNA MIR4435-2HG targets desmoplakin and promotes growth and metastasis of gastric cancer by activating Wnt/β-catenin signaling. Aging (Albany NY) 2019;11:6657-73.
27. Cai H, Liang J, Jiang Y, et al. Integrative Analysis of N6-Methyladenosine-Related Enhancer RNAs Identifies Distinct Prognosis and Tumor Immune Micro-Environment Patterns in Head and Neck Squamous Cell Carcinoma. Cancers (Basel) 2022;14:4657.
28. Xing P, Wang Y, Zhang L, et al. Knockdown of lncRNA MIR4435-2HG and ST8SIA1 expression inhibits the proliferation, invasion and migration of prostate cancer cells in vitro and in vivo by blocking the activation of the FAK/AKT/β-catenin signaling pathway. Int J Mol Med 2021;47:93.
29. Bin Wang, Yuan C, Qie Y, et al. Long non-coding RNAs and pancreatic cancer: A multifaceted view. Biomed Pharmacother 2023;167:115601.
30. Salmena L, Poliseno L, Tay Y, et al. A ceRNA hypothesis: the Rosetta Stone of a hidden RNA language? Cell 2011;146:353-8.
31. Tay Y, Rinn J, Pandolfi PP. The multilayered complexity of ceRNA crosstalk and competition. Nature 2014;505:344-52.
32. Shen X, Ding Y, Lu F, et al. Long noncoding RNA MIR4435-2HG promotes hepatocellular carcinoma proliferation and metastasis through the miR-22-3p/YWHAZ axis. Am J Transl Res 2020;12:6381-94.
33. Zhu K, Miao C, Tian Y, et al. lncRNA MIR4435-2HG promoted clear cell renal cell carcinoma malignant progression via miR-513a-5p/KLF6 axis. J Cell Mol Med 2020;24:10013-26.
34. Yu M, Yi Z, Chen S, et al. MIR4435-2HG, miR-125b-5p, and Sema4D axis affects the aggressiveness of colorectal cancer cells. Folia Histochem Cytobiol 2022;60:191-202.
35. Dong X, Yang Z, Yang H, et al. Long Non-coding RNA MIR4435-2HG Promotes Colorectal Cancer Proliferation and Metastasis Through miR-206/YAP1 Axis. Front Oncol 2020;10:160.
36. Xu H, Zhang B, Yang Y, et al. LncRNA MIR4435-2HG potentiates the proliferation and invasion of glioblastoma cells via modulating miR-1224-5p/TGFBR2 axis. J Cell Mol Med 2020;24:6362-72.
37. Gao LF, Li W, Liu YG, et al. Inhibition of MIR4435-2HG on Invasion, Migration, and EMT of Gastric Carcinoma Cells by Mediating MiR-138-5p/Sox4 Axis. Front Oncol 2021;11:661288.
38. Han L, Xiong L, Wang C, et al. MicroRNA-128 contributes to the progression of gastric carcinoma through GAREM-mediated MAPK signaling activation. Biochem Biophys Res Commun 2018;504:295-301.
39. Khadka VS, Nasu M, Deng Y, et al. Circulating microRNA Biomarker for Detecting Breast Cancer in High-Risk Benign Breast Tumors. Int J Mol Sci 2023;24:7553.
40. Nalla LV, Khairnar A. Empagliflozin mediated miR-128-3p upregulation promotes differentiation of hypoxic cancer stem-like cells in breast cancer. Eur J Pharmacol 2023;943:175565.
41. Frixa T, Sacconi A, Cioce M, et al. MicroRNA-128-3p-mediated depletion of Drosha promotes lung cancer cell migration. Carcinogenesis 2018;39:293-304.
42. Mustafov D, Karteris E, Braoudaki M. Deciphering the Role of microRNA Mediated Regulation of Coronin 1C in Glioblastoma Development and Metastasis. Noncoding RNA 2023;9:4.
43. Zhang Y, Guo S, Wang S, et al. LncRNA OIP5-AS1 inhibits ferroptosis in prostate cancer with long-term cadmium exposure through miR-128-3p/SLC7A11 signaling. Ecotoxicol Environ Saf 2021;220:112376.
44. Kim K, Yoo D, Lee HS, et al. Identification of potential biomarkers for diagnosis of pancreatic and biliary tract cancers by sequencing of serum microRNAs. BMC Med Genomics 2019;12:62.
45. Wang B, Sun X, Huang KJ, et al. Long non-coding RNA TP73-AS1 promotes pancreatic cancer growth and metastasis through miRNA-128-3p/GOLM1 axis. World J Gastroenterol 2021;27:1993-2014.
46. Zheng T, Han W, Wang A, et al. Functional mechanism of hsa-miR-128-3p in epithelial-mesenchymal transition of pancreatic cancer cells via ZEB1 regulation. PeerJ 2022;10:e12802.
47. Lin DT, Conibear E. ABHD17 proteins are novel protein depalmitoylases that regulate N-Ras palmitate turnover and subcellular localization. Elife 2015;4:e11306.
48. Del Rivero Morfin PJ, Ben-Johny M. Cutting out the fat: Site-specific deacylation of an ion channel. J Biol Chem 2020;295:16497-8.
49. Chen L, Pan X, Zhang YH, et al. Primary Tumor Site Specificity is Preserved in Patient-Derived Tumor

Xenograft Models. Front Genet 2019;10:738.
50. Zheng Q, Fang W, Huang Y, et al. Identification of a Novel KIF5B-RET, ABHD17C-RET Double-Fusion Variant in Lung Adenocarcinoma and Response to Cabozantinib. J Thorac Oncol 2020;15:e132-3.
51. Jiang F, Huang X, Zhang F, et al. Integrated Analysis of Multi-Omics Data to Identify Prognostic Genes for Pancreatic Cancer. DNA Cell Biol 2022;41:305-18.

Cite this article as: Chen Z, Du Y, Shi H, Dong S, He R, Zhou W. Long non-coding RNA MIR4435-2HG promotes pancreatic cancer progression by regulating ABHD17C through sponging miR-128-3p. Transl Cancer Res 2024;13(8):4113-4130. doi: 10.21037/tcr-24-51

